

## Excitation of Multiple-Magnon Bound States in $\text{CoCl}_2 \cdot 2\text{H}_2\text{O}^\dagger$

J. B. TORRANCE, Jr.,\* and M. TINKHAM

*Division of Engineering and Applied Physics, Harvard University, Cambridge, Massachusetts 02138*

(Received 23 June 1969)

The results of far-infrared transmission measurements on  $\text{CoCl}_2 \cdot 2\text{H}_2\text{O}$  at helium temperatures are reported and compared with theoretical predictions. Antiferromagnetic resonance, ferrimagnetic resonance, and ferromagnetic resonance have been observed in the respective metamagnetic phases of this material. Furthermore, these magnons appear to interact with an unexpected excitation which is believed to be an optical phonon. The most striking feature of the data, however, is the appearance of absorption lines in each phase which shift with magnetic field at a rate corresponding to  $g$  values of about 14, 21, 28, and even 35, as compared to the  $g$  value of  $\sim 7$  for the single magnons. Furthermore, the energy of each of these  $n$ -fold multiple excitations is markedly less than  $n$  times the energy of a onefold one. These excitations are identified as clustered spin reversals or magnon bound states, and this is the first direct observation of such states. In the simple Ising-model approximation, such clusters of  $n$  adjacent spin reversals are eigenstates, and the Ising-model energies qualitatively describe the observed energy spectra in all three phases. Using the theoretical results of the preceding paper, the small non-Ising terms are included in the theory, and excellent quantitative agreement is obtained. The reasons why bound states can be observed in  $\text{CoCl}_2 \cdot 2\text{H}_2\text{O}$  are also discussed.

### INTRODUCTION

MANY of the features of the observed far infrared absorption spectrum<sup>1,2</sup> of  $\text{CoCl}_2 \cdot 2\text{H}_2\text{O}$  may be understood by considering a simple model: the ferromagnetic Ising linear chain with  $S = \frac{1}{2}$ . The elementary excitations of such a chain are spin clusters, where an  $n$ -fold spin cluster is defined as  $n$  adjacent spins which are reversed with respect to the majority of the spins in the chain.<sup>3</sup> The increased exchange energy  $2J_0^{zz}$ , associated with creating an  $n$ -fold cluster according to the Ising model, is localized at the ends of the cluster and is, therefore, independent of its length. In the presence of an external magnetic field, there is a Zeeman energy associated with each spin in the  $n$ -fold cluster. Hence, the total energy  $E_n$  necessary to excite an  $n$ -fold cluster is given by

$$E_n = 2J_0^{zz} + ng_{11}\mu_B H_0, \quad (1)$$

where the external field  $H_0$  is along the axis of magnetization  $z$  and the corresponding spectroscopic splitting factor is  $g_{11}$ . These excitations are characterized by the fact that in weak fields  $E_n$  is much less than  $n$  times the energy  $E_1$  required to create a single spin excitation.

In a ferromagnetic linear chain where the exchange interaction has finite transverse components, the  $n$ -fold excitations corresponding to spin clusters no longer contain only adjacent spin reversals (as in the

Ising model). In this case the excitation is more appropriately described as a packet of  $n$  spatially correlated or clustered spin reversals, which form a bound state.<sup>4-6</sup> It is not possible to account for these bound states using linear or noninteracting spin-wave theory,<sup>7</sup> since, from this point of view, it is the (attractive) interaction between spin waves, or magnons, which gives rise to the binding energy, so that the energy of an  $n$ -magnon bound state is less than the energy of  $n$  noninteracting magnons. In two and three dimensions, such bound states generally exist only near the zone boundary,<sup>5</sup> and in all cases they are difficult to observe. In this paper we present a detailed analysis of the first direct observation<sup>1</sup> of these magnon bound states, using the results of the theory developed in the preceding paper.<sup>6</sup>

### MAGNETIC PROPERTIES OF $\text{CoCl}_2 \cdot 2\text{H}_2\text{O}$

The crystal structure of  $\text{CoCl}_2 \cdot 2\text{H}_2\text{O}$  (CC2) is monoclinic, with a twofold axis ( $b$ ) and a mirror plane ( $a$ - $c$ ).<sup>8</sup> The  $\text{Co}^{++}$  ions form linear— $\text{CoCl}_2$ —chains along the  $c$  axis. The exchange interaction  $J_0$  between  $\text{Co}^{++}$  spins within the same chain is ferromagnetic ( $F_0$ ) and much stronger than the interactions between chains.<sup>9</sup> Furthermore, the exchange interactions have extreme longitudinal anisotropy, with an "easy"  $b$

<sup>4</sup> H. A. Bethe, *Z. Physik* **71**, 205 (1931); R. Orbach, *Phys. Rev.* **112**, 309 (1958).

<sup>5</sup> M. Wortis, *Phys. Rev.* **132**, 85 (1963); N. Fukuda and M. Wortis, *J. Phys. Chem. Solids* **24**, 1675 (1963); J. Hanus, *Phys. Rev. Letters* **11**, 336 (1963); J. G. Hanus, *Quart. Progr. Rept. Solid State Mol. Theory Group (MIT)* **43**, 96 (1962); **44**, 38 (1962); **46**, 137 (1962).

<sup>6</sup> J. B. Torrance, Jr., and M. Tinkham, preceding paper, *Phys. Rev.* **187**, 587 (1969).

<sup>7</sup> See, e.g., F. Keffer, in *Handbuch der Physik* (Springer-Verlag, Berlin, 1966), Vol. 18.

<sup>8</sup> B. K. Vainshtein, *Dokl. Akad. Nauk, SSSR* **68**, 301 (1949); **83**, 227 (1952); B. Morosin and E. J. Graeber, *Acta Cryst.* **16**, 1176 (1963).

<sup>9</sup> H. Kobayashi and T. Haseda, *J. Phys. Soc. Japan* **19**, 765 (1964).

<sup>†</sup> Work partially supported by the National Science Foundation, Advanced Research Projects Agency, and the Office of Naval Research.

\* Present address: IBM Research Center, Yorktown Heights, N. Y.

<sup>1</sup> J. B. Torrance, Jr., and M. Tinkham, *J. Appl. Phys.* **39**, 822 (1968); *Bull. Am. Phys. Soc.* **13**, 390 (1968).

<sup>2</sup> J. B. Torrance, Jr., Ph.D. thesis, Harvard University, 1968 (unpublished); Harvard University, Division of Engineering and Applied Physics, Technical Report No. 1, 1969 (unpublished).

<sup>3</sup> M. Date and M. Motokawa, *Phys. Rev. Letters* **16**, 1111 (1956); *J. Phys. Soc. Japan* **24**, 41 (1968).

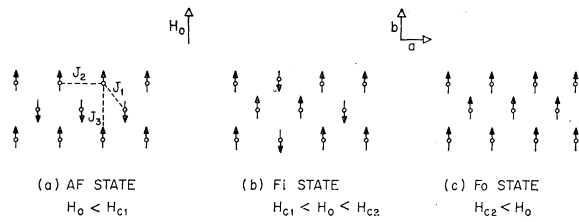


FIG. 1. (a) Antiferromagnetic (AF); (b) ferrimagnetic (Fi); and (c) ferromagnetic (Fo) spin structures of  $\text{CoCl}_2 \cdot 2\text{H}_2\text{O}$  for the external magnetic field  $H_0$  along the  $b$  axis. This figure shows a cross section through the chains of spins, which are coming out of the plane of the figure.

axis. It is because of this strong anisotropy that we are able to regard the individual chains of spins in CC2 as Ising-like chains, where the spins are either up or down with respect to the  $b$  axis.

Neighboring chains are weakly bonded by the waters of hydration. The exchange interactions between different chains are correspondingly weak. These interactions are predominantly antiferromagnetic and tend to order the spins of a particular Fo chain antiparallel to those of neighboring chains. Below  $T_N (= 17.2^\circ\text{K})$ ,<sup>10</sup> CC2 is a two sublattice antiferromagnet (AF), as shown in Fig. 1(a).<sup>11,12</sup> This figure represents a typical cross section through the chains of spins that are coming out of the plane of the figure. The exchange interactions between chains are also shown:  $J_1$  and  $J_2$  are antiferromagnetic, while  $J_3$  is ferromagnetic, but extremely small.

For large external magnetic fields along the axis of magnetization ( $b$  axis), the Zeeman energy of a spin becomes comparable to the *interchain* exchange energies. It may then become energetically favorable for the chains of spins to reorient. Thus, for  $T \ll T_N$ , at  $H_0 = H_{C1} = 31.3$  kOe there is a transition to a ferromagnetic (Fi) spin structure [Fig. 1(b)] and at  $H_0 = H_{C2} = 44.9$  kOe there is a second metamagnetic transition to the ferromagnetic (Fo) arrangement of Fig. 1(c).<sup>13-15</sup> These transition fields may be related to the interchain exchange interactions by<sup>16</sup>

$$\begin{aligned} g_{11}\mu_B H_{C1} &= p_1 |J_1^{zz}| - 2p_2 |J_2^{zz}|, \\ g_{11}\mu_B H_{C2} &= p_1 |J_1^{zz}| + p_2 |J_2^{zz}|, \end{aligned} \quad (2)$$

where  $p_i$  is the coordinate number of the exchange  $J_i$ . For  $p_1 = 4$  and  $p_2 = 2$ , we obtain  $|J_1^{zz}| = 3.52 \text{ cm}^{-1}$  and

<sup>10</sup> T. Shinoda, H. Chihara, and S. Seki, *J. Phys. Soc. Japan* **19**, 1637 (1964).

<sup>11</sup> A. Narath, *Phys. Rev.* **136**, A766 (1964).

<sup>12</sup> D. E. Cox, B. C. Frazer, and G. Shirane, *Phys. Letters* **17**, 103 (1965).

<sup>13</sup> The field-dependent magnetization behavior of  $\text{CoCl}_2 \cdot 2\text{H}_2\text{O}$  was discovered independently by A. Narath and D. Barham [*Bull. Am. Phys. Soc.* **9**, 112 (1964)] and H. Kobayashi and T. Haseda [*J. Phys. Soc. Japan* **19**, 765 (1964)].

<sup>14</sup> Values of  $H_{C1}$  and  $H_{C2}$  are taken from the most recent measurements: A. Narath and J. E. Shirber, *J. Appl. Phys.* **37**, 1124 (1966). Values of  $H_{C1} = 31.6$  and  $31.8$  kOe and  $H_{C2} = 46.0$  kOe have also been reported.

<sup>15</sup> D. E. Cox, G. Shirane, B. C. Frazer, and A. Narath, *J. Appl. Phys.* **37**, 1126 (1966).

<sup>16</sup> A. Narath, *Phys. Letters* **13**, 12 (1964).

$|J_2^{zz}| = 0.7 \text{ cm}^{-1}$ , as compared to the value<sup>1</sup> of  $J_0^{zz} = 12.7 \text{ cm}^{-1}$ . The fact that CC2 exhibits these metamagnetic transitions, as opposed to the more common spin-flop transition, is due to the strong longitudinal anisotropy of this material.<sup>2</sup>

Since the orbital angular momentum of the  $\text{Co}^{++}$  ion is not completely quenched, the anisotropic crystal field of CC2 may act on the spin via the spin-orbit coupling. This causes the exchange and Zeeman energies to become anisotropic, i.e., causes them to depend on the orientation of the spins and the magnetic field with respect to the crystal axis. In CC2 the anisotropy is sufficiently strong that it is convenient to introduce a fictitious isotropic spin ( $S = \frac{1}{2}$ ) and confine this anisotropy to effective  $g$  values and exchange interactions. If we assume that the original exchange  $J'$  is isotropic in the true spin, the resulting anisotropies in these tensors are related by<sup>2,17</sup>

$$(g_s^{\alpha\alpha})^2 J' = 4J^{\alpha\alpha}, \quad (3)$$

where  $J^{\alpha\alpha}$  and  $g_s^{\alpha\alpha}$  are the principal values of the exchange tensor and spin part of the  $g$  tensor, respectively.

From a detailed crystal field analysis of his susceptibility data, Narath<sup>18</sup> has obtained the energies and  $g$  values for the lowest six Kramers doublets. Using (3) and the spin part of the  $g$  tensor for the lowest doublet, we may obtain a measure of the anisotropy to be expected in each of the exchange interactions

$$J^{zz}/J^{xx}/J^{yy} = 7.3/2.1/1.0. \quad (4)$$

In practice, however, the situation is usually more complicated and it is unrealistic to expect quantitative agreement with the above discussion.

## EXPERIMENTAL TECHNIQUES

### Monochromator

The grating monochromator used in these experiments is shown schematically in Fig. 2.<sup>19</sup> The source of broad band far infrared radiation<sup>20</sup> is a high-pressure mercury arc lamp (G.E. UA-3), which is housed in the mirror  $M_1$ . This lamp is cooled indirectly by water circulating through a plate on the outside of the vacuum tank. The spherical mirrors  $M_1$  and  $M_2$  and the (annular) zero-order filter gratings form the on-axis source optics.<sup>21</sup> In the second stage,  $M_3$ ,  $M_4$ , and the main grating are arranged in the Czerny-Turner

<sup>17</sup> I. F. Silvera, J. H. M. Thornley, and M. Tinkham, *Phys. Rev.* **136**, A695 (1964).

<sup>18</sup> A. Narath, *Phys. Rev.* **140**, A552 (1965).

<sup>19</sup> A number of people were involved in the construction of the monochromator: K. A. Hay, R. S. Newbower, J. M. Peech, T. Penney, R. Rex, P. C. L. Tai, and P. R. Wyder, in addition to the authors.

<sup>20</sup> *Spectroscopic Techniques for Far-Infrared, Submillimetre, and Millimetre Waves*, edited by D. H. Martin (North-Holland Publishing Co., Amsterdam, 1967); A. Hadni, *Essentials of Modern Physics Applied to the Study of the Infrared* (Pergamon Press, Inc., New York, 1967); E. D. Palik, NRL Bibliography No. 21, AF-407047, 1963 (unpublished) (also first supplement to a far infrared bibliography, 1965).

<sup>21</sup> The source optics are based on a design by L. H. Palmer.

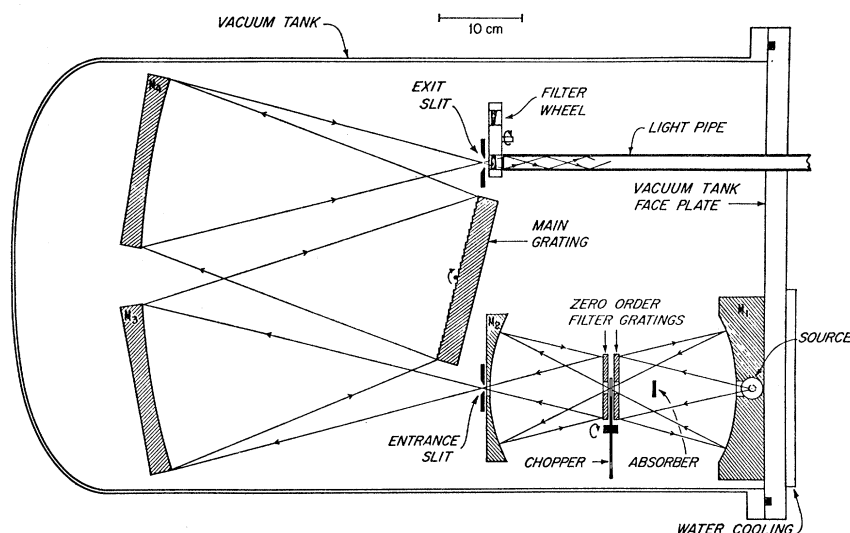


FIG. 2. A schematic diagram of the monochromator and optical path.

geometry with an  $f/2.0$  aperture. The “absorber” prohibits radiation from passing directly from the lamp to the entrance slit without first being filtered by the zero-order gratings. This filtering is necessary to reduce the intensity of the higher harmonics of the desired frequency. In this geometry, zero-order gratings blazed at  $27^\circ$  are observed to have particularly sharp cutoffs.<sup>2</sup> Yoshinaga filters<sup>20,22</sup> as well as crystal quartz are also used and are mounted in the transmission filter wheel.

During the final phases of this work, a signal processing system (Fig. 3) was designed and constructed by R. S. Newbower and P. C. L. Tai. This system enabled the spectra to be punched directly on IBM cards and then analyzed by a computer.<sup>2</sup> The data from a given run could be further smoothed by the computer and/or ratioed against another spectrum. The output was plotted versus frequency or grating angle by a Cal Comp plotter.

#### Low-Temperature Apparatus

The object of the experiment was to measure the far infrared transmission spectrum of  $\text{CoCl}_2 \cdot 2\text{H}_2\text{O}$  at pumped-helium temperatures and in high magnetic fields. For this reason, a cryostat was constructed to be used with a 55-kOe superconducting solenoid. Figure 4 shows a schematic diagram of this apparatus with a detailed cross section of the lower portion. Far infrared radiation from the monochromator enters the top of the apparatus and is conveyed by brass light pipe to the sample. It then passes through the sample and up a final section of light pipe to the bolometer. When used, a far infrared polarizer<sup>23</sup> is placed next to the sample in the gap of the light pipe.

<sup>22</sup> The Yoshinaga filters used were kindly given to us by Dr. I. F. Silvera.

<sup>23</sup> The polarizer consisted of gold lines deposited on Mylar. These are manufactured by Buckbee-Mears Co., St. Paul, Minnesota, and described by I. F. Silvera and J. Woods Halley, *Phys. Rev.* **149**, 415 (1966).

For transmission experiments it is desirable to have the sample in the form of a plate. Since the crystals are long in the  $c$  direction, it is convenient to have the  $c$  axes in the plane of the sample. The effects of demagnetizing fields in the ferromagnetic and ferrimagnetic states are greatly reduced by choosing the axis of magnetization ( $b$  axis) as the other axis in the plane of the sample. In order to ensure good thermal contact over the whole sample, the crystal is cemented with G.E. 7031 varnish to a wedged quartz substrate. (At helium temperatures quartz is transparent in the far infrared and is a good thermal conductor.) The substrate is then glued to a copper rod, which is soldered to the copper braid that leads to the helium can. The end of this braid is soldered to a  $1\text{-cm}^2$  plate which is screwed down to the bottom of the helium can with a thin layer of Apiezon  $N$  grease between them [Fig. 4(b)]. The sample could be cooled to  $\lesssim 1.6^\circ\text{K}$ , as compared to the helium bath temperature of  $1.1^\circ\text{K}$ .

The sample is usually mounted with the (vertical) magnetic field along the axis of magnetization or  $b$

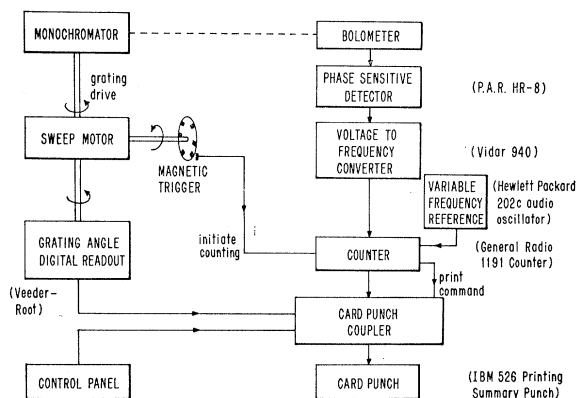


FIG. 3. The signal processing system used to digitize the data. The card-punch coupler was designed and built by R. S. Newbower.

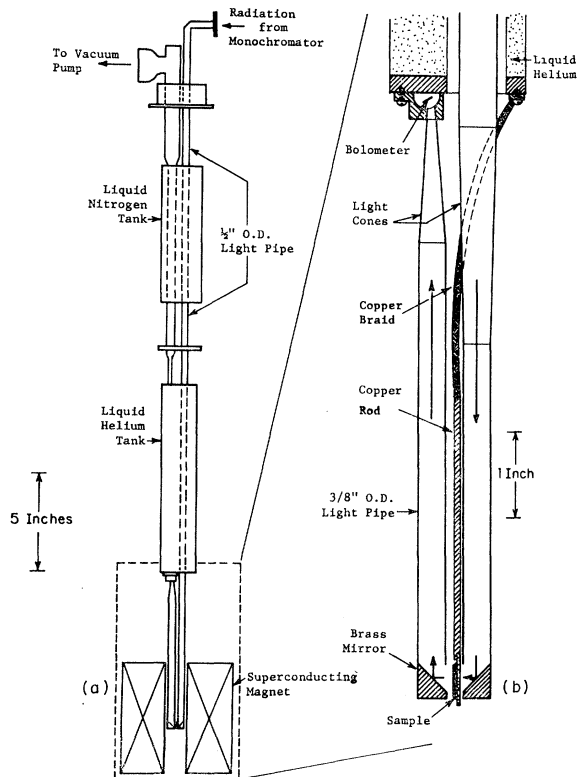


FIG. 4. A schematic diagram of (a) the low-temperature apparatus used in these experiments and (b) a cross section of the lower portion of (a).

axis, as in Fig. 4(b). This geometry has the added advantage that absorption of radiation polarized both parallel and perpendicular to the  $b$  axis may be observed. Another geometry (not shown) enables absorption of radiation polarized in the  $a$ - $c$  plane to be measured.

### Crystals

Single crystals of  $\text{CoCl}_2 \cdot 2\text{H}_2\text{O}$  were grown by slow evaporation of a saturated solution at  $70^\circ\text{C}$ .<sup>11</sup> A regulated oil bath inside a regulated oven kept hourly drifts and variations of the bath temperature below  $0.02^\circ\text{C}$  throughout the growth period (typically one month). The crystals were oriented from their morphology<sup>2</sup> and checked by x-ray back reflection. No evidence of twinning was found.

### EXPERIMENTAL RESULTS

The observed absorption frequencies are plotted versus the applied magnetic field in Figs. 5(a) and 6. Measurements were taken from 0–55 kOe and from 15–145  $\text{cm}^{-1}$ , where the sample became opaque (presumably due to absorption by optical phonons). The metamagnetic transitions are indicated by the lines which terminate at  $H_{C1}$  and  $H_{C2}$ . The resonance frequencies observed at zero field are 29.15, 31.05, 34.9, 47.8, and 59.7  $\text{cm}^{-1}$  (all frequencies are  $\pm 0.1 \text{ cm}^{-1}$ ).

These results agree with the work of Silveira,<sup>24</sup> who made the first far infrared measurements on  $\text{CoCl}_2 \cdot 2\text{H}_2\text{O}$  (CC2). His measurements were limited, however, to magnetic fields less than 11 kOe and only the lines labeled  $b_1$ ,  $ph$ ,  $a_1$ ,  $b_2$ , and  $a_2$  could be observed.

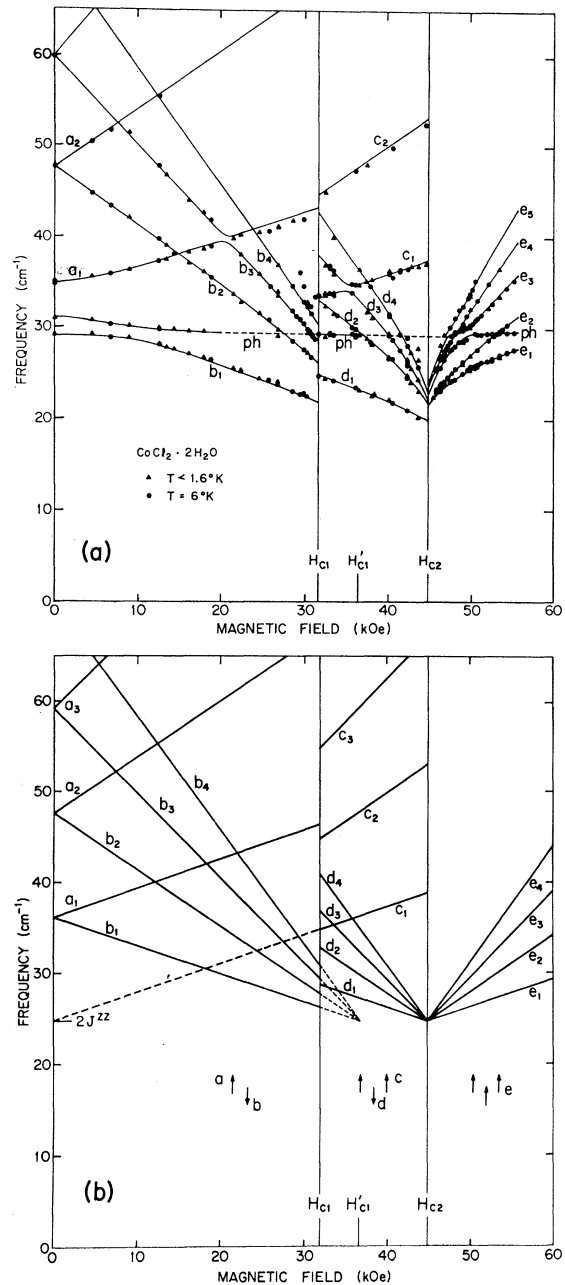
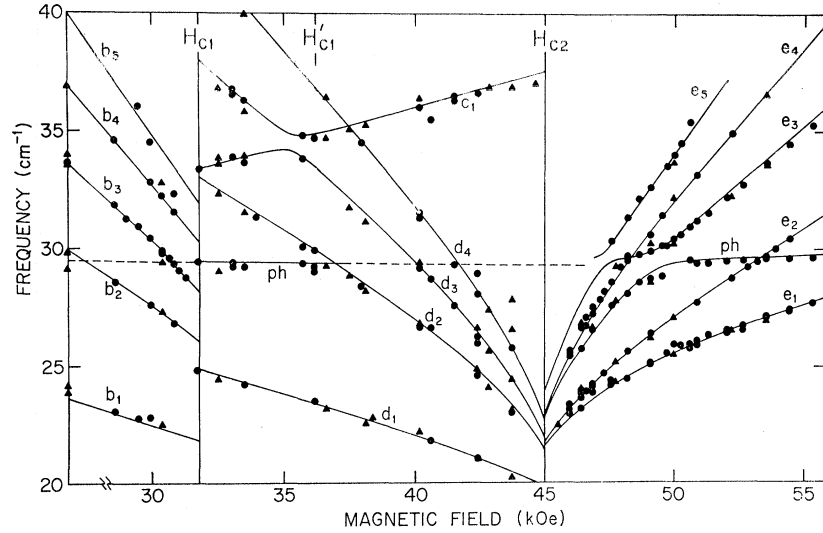


FIG. 5. (a) The observed resonance frequencies are plotted against the magnetic field  $H_0$ , which is applied along the  $b$  axis. Measurements were taken at  $T \lesssim 1.6^\circ\text{K}$  (triangles) and  $T = 6^\circ\text{K}$  (circles). The lines are the results of detailed theoretical calculations. (b) The simple Ising-model excitation spectra for spin clusters in the chains of  $\text{CoCl}_2 \cdot 2\text{H}_2\text{O}$ .

<sup>24</sup> I. F. Silveira, Ph.D. thesis, University of California, Berkeley, 1965 (unpublished).

Fig. 6. A detailed comparison of theory (lines) with experiment (points) for  $\text{CoCl}_2 \cdot 2\text{H}_2\text{O}$  between 20 and 40  $\text{cm}^{-1}$ .



Silvera showed that these lines broadened with increasing temperature and slowly shifted to a lower frequency as the Néel temperature ( $17.2^\circ\text{K}$ ) was approached. For  $T < 6^\circ\text{K}$ , however, there is very little change in the resonances. This temperature independence is illustrated in Figs. 5(a) and 6, where the triangles represent data taken at  $T \lesssim 1.6^\circ\text{K}$  and the circles correspond to  $T = 6^\circ\text{K}$  data.

A brief qualitative examination of Figs. 5(a) and 6 reveals the major feature of the data: the presence of sets of absorption lines in each phase with slopes corresponding to  $2g$ ,  $3g$ , and  $4g$  as well as the expected  $g$  value. If we concentrate on the ferromagnetic (Fo) region, for example, we find the set labeled  $e_1$ ,  $e_2$ ,  $e_3$ ,  $e_4$ , and  $e_5$ . Line  $e_1$  has a slope corresponding to the expected  $g$  value of about seven; it presumably corresponds to some type of *single* spin excitation, such as ferromagnetic resonance. On the other hand,  $e_2$  has a slope corresponding to a  $g$  value of approximately 14, or twice the expected value. This *slope* suggests that it is associated with some types of a double spin excitation. Furthermore, the energy of this "double" level is larger than  $e_1$ , but much less than twice as large. Therefore,  $e_2$  cannot simply be attributed to the simultaneous creation of two *independent* excitations of the type  $e_1$ , as that would require an energy of about  $50 \text{ cm}^{-1}$ . Line  $e_2$  is also about one-third as intense as  $e_1$ .

A similar situation exists for  $e_3$ ,  $e_4$ , and  $e_5$ , which have slopes corresponding to  $g$  values of 21, 28, and 35 and have even weaker intensities. (If higher levels existed, their intensities were too weak to detect.) In the other regions there are similar sets, labeled  $a$ ,  $b$ ,  $c$ , and  $d$  in Figs. 5(a) and 6.

The interpretation is that not only have *single* spin excitations been observed, but also multiple excitations. Furthermore, the spins in these multiple excitations are somehow coupled, correlated, or clustered, so that the energy to excite an  $n$ -fold spin excitation is much

less than  $n$  times the energy to create a single excitation. These properties suggest that the excitations correspond to magnon bound states.

## THEORY

### Ising Model

The spin system in  $\text{CoCl}_2 \cdot 2\text{H}_2\text{O}$  (CC2) is assumed to be described by the following exchange Hamiltonian:

$$\mathcal{H} = - \sum_{i,\delta} \{ J_{\delta}^{zz} S_i^z S_{i+\delta}^z + J_{\delta}^{xx} S_i^x S_{i+\delta}^x + J_{\delta}^{yy} S_i^y S_{i+\delta}^y \} - \sum_i g_{11} \mu_B H_0 S_i^z, \quad (5)$$

where the exchange interaction  $J_{\delta}$  couples  $\mathbf{S}_i$  to  $\mathbf{S}_{i+\delta}$ . It is convenient to decompose this Hamiltonian as follows:

$$\mathcal{H} = \mathcal{H}^I + \mathcal{H}^{\perp} + \mathcal{H}^a, \quad (6)$$

where

$$\mathcal{H}^I \equiv - \sum_{i,\delta} J_{\delta}^{zz} S_i^z S_{i+\delta}^z - \sum_i g_{11} \mu_B H_0 S_i^z, \quad (7)$$

$$\mathcal{H}^{\perp} \equiv - \sum_{i,\delta} \frac{J_{\delta}^{\perp}}{2} (S_i^+ S_{i+\delta}^- + S_i^- S_{i+\delta}^+), \quad (8)$$

and

$$\mathcal{H}^a \equiv - \sum_{i,\delta} \frac{J_{\delta}^a}{2} (S_i^+ S_{i+\delta}^+ + S_i^- S_{i+\delta}^-), \quad (9)$$

with

$$S^{\pm} = S^x \pm iS^y, \quad J_{\delta}^{\perp} \equiv \frac{J_{\delta}^{xx} + J_{\delta}^{yy}}{2}, \quad J_{\delta}^a \equiv \frac{J_{\delta}^{xx} - J_{\delta}^{yy}}{2}.$$

Due to the large longitudinal anisotropy

$$[(J^{\perp})^2 \ll (J^{zz})^2]$$

in CC2,<sup>25</sup> it is a reasonable first approximation to

<sup>25</sup> T. Oguchi, J. Phys. Soc. Japan **20**, 2236 (1965).

neglect  $\mathfrak{J}C_1$  and  $\mathfrak{J}C^a$ , leaving the Ising-model Hamiltonian (7). In this case, it is convenient to picture each chain in CC2 as an isolated ferromagnetic chain. The interactions with neighboring chains may then be represented by an internal field  $H_{\text{int}}$ , so that the energy required to create an  $n$ -fold cluster on one of these chains is [from (1)]

$$E_n = 2J_0^{zz} + ng_{11}\mu_B(H_0 + H_{\text{int}}). \quad (10)$$

The internal field  $H_{\text{int}}$ , due to interchain exchange interactions, may be calculated using (7) and the spin structures of CC2 (Fig. 1). If  $J_3$  is neglected, the resulting excitation energies are

$$\begin{aligned} \text{AF state: } hv_{a,n} &= p_0 J_0^{zz} + ng_{11}\mu_B(H_{C1}' + H_0), \\ hv_{b,n} &= p_0 J_0^{zz} + g_{11}\mu_B(H_{C1}' - H_0), \\ \text{Fi state: } hv_{c,n} &= p_0 J_0^{zz} + ng_{11}\mu_B H_0, \\ hv_{d,n} &= p_0 J_0^{zz} + ng_{11}\mu_B(H_{C2} - H_0), \\ \text{Fo state: } hv_{e,n} &= p_0 J_0^{zz} + ng_{11}\mu_B(H_0 - H_{C2}). \end{aligned} \quad (11)$$

The subscripts  $a, b, c, d$ , and  $e$  identify the chains on which the clusters are created, e.g., line  $b_3$  corresponds to the creation of a threefold cluster on a down chain in the AF phase. In (11) we have used the relations (2) to express  $|J_1^{zz}|$  and  $|J_2^{zz}|$  in terms of  $H_{C1}$ ,  $H_{C2}$ , and  $H_{C1}'$ , which is defined as follows:

$$g_{11}\mu_B H_{C1}' = p_1 |J_1^{zz}| - p_2 |J_2^{zz}| = g_{11}\mu_B \frac{2H_{C1} + H_{C2}}{3}. \quad (12)$$

The results for  $n=1, 2, 3$ , and 4 are shown in Fig. 5(b). These energies are uniquely determined by values for  $g_{11}$ ,  $H_{C1}$ ,  $H_{C2}$ , and  $p_0 J_0^{zz}$ . The experimental values for  $H_{C1}$  (31.3 kOe) and  $H_{C2}$  (44.9 kOe), and fitted values of  $g_{11}$  (6.8) and  $p_0 J_0^{zz}$  (24.5  $\text{cm}^{-1}$ ) have been used. ( $p_0 J_0^{zz}$  fixes the zero of energy and the slope is fixed by  $g_{11}$ .)

The theoretical spectrum of Fig. 5(b) represents a superposition of the spectra for different chains, each of which senses a different internal field  $H_{\text{int}}$ . In the AF region, for example, there are two sets of lines— $a$  and  $b$  of Fig. 5. These correspond to creating clusters on the up and down chains, respectively. Similarly, the  $c$  lines and  $d$  lines correspond to cluster creation on the up and down chains in the Fi region. Since there are twice as many up chains as down chains in this region, it would be expected, for example, that the absorption intensity of  $c_1$  would be twice as strong as  $d_1$ ; this is generally observed.

In the Fo region there is only one set of lines since all of the chains are up. The fact that the  $e$  lines converge at  $H_{C2}$  indicates that, at that point, the external field is exactly cancelled by the (antiferromagnetic) exchange field due to neighboring chains. Each chain sees, therefore, an internal field equal to  $-H_{C2}$ . The same is true for the down chains in the Fi phase, since the  $d$  lines also converge at  $H_{C2}$ . It is no coincidence that  $H_{C2}$  is the transition field: When  $H_0 = H_{C2} - h$ , the

$d$  chains see a net field equal to  $-h$ , aligning them downward; for  $H_0 = H_{C2}$ , they sense no net field; but for  $H = H_{C2} + h$  the down chains see a field  $+h$  and reverse themselves to align with the field, taking the crystal into the Fo phase.

A comparison of this result with the experimental spectrum of Fig. 5(a) reveals remarkable agreement for such a simple model. The existence of the major lines are accounted for as well as their approximate frequencies. Some information about their intensities is also obtained. In addition, this model is able to give a physical interpretation to the observed spectrum. The substantial agreement makes it possible to identify these excitations as spin clusters or magnon bound states, and these experiments constitute the first direct observation of such excitations in any material.

There are, however, significant departures from this simple theory, which are conveniently divided into three classes:

(1) Absorption lines are observed which are not predicted by the theory. For example,  $ph$  labels a line at about  $30 \text{ cm}^{-1}$  which is observed in each region. Furthermore,  $ph$  appears to interact with the expected excitations. Absorption is also observed<sup>1</sup> (but not shown in Figs. 5 or 6), which is associated with lines which appear to “persist” beyond the transition fields.

(2) The energy of certain lines is shifted down from the Ising predictions. In the Fi phase, for example, the energy of  $d_1$  at  $H_{C2}$  is approximately  $3 \text{ cm}^{-1}$  lower than the energy of  $d_2, d_3$ , and  $d_4$ .

(3) In many parts of the spectrum, the lines have considerable curvature, particularly near  $H_{C2}$  (Fig. 6). The apparent  $g$  values (defined by a local slope) are observed to vary from 6.4 to 7.3. Also, lines  $a_1$  and  $b_1$  are strongly interacting near zero field. Associated with this type of discrepancy is another problem: How is it possible to excite these multiple excitations? The excitation of an  $n$ -magnon bound state corresponds to a  $\Delta m = n$  transition, normally forbidden for  $n > 1$ .

The latter two classes of discrepancies are associated with the non-Ising terms, Eqs. (8) and (9), in the Hamiltonian, which must be included in a more exact theory. The theoretical approach developed in detail in the preceding paper<sup>6</sup> is to start with the Ising solution [Fig. 5(b)] and then consider the effects of  $\mathfrak{J}C^1$  and  $\mathfrak{J}C^a$  on that solution.

#### Phonon and Persisting Lines

In each of the three metamagnetic phases, there appears an absorption line, labeled  $ph$  in Figs. 5(a) and 6, which is not accounted for by the Ising model. The major feature of this new line is that, when compared to the other excitations, its energy is relatively field-independent. Furthermore, its slight field dependence appears to be due to interaction with the magnetic excitations. This excitation and its interactions are

described in more detail elsewhere,<sup>26</sup> together with the observation of a similar excitation in  $\text{FeCl}_2 \cdot 2\text{H}_2\text{O}$ . There it is argued that  $ph$  is an optical phonon, which is infrared active only due to its interaction with the magnons. The experimental data on both materials are well described by assuming that the phonon with energy  $E_{ph}$  interacts with the spin waves via a phenomenological magnon-phonon coupling. This coupling is included as an off-diagonal matrix element  $A$  in the theoretical calculations described in the next section.

At  $T \lesssim 1.6^\circ\text{K}$ , the line labeled  $c_1$  in Fig. 5(a) in the ferrimagnetic (Fi) state, appears to persist beyond  $H_{C1}$  into the antiferromagnetic (AF) state, i.e., weak absorption is observed in the AF region at points which would fall on  $c_1$  if it were extended beyond  $H_{C1}$ . [This absorption is not shown in Figs. 5(a) or 6, but is shown in Ref. 1]. It is also observed that the AF lines  $a_1$  and  $b_1$  persist into the Fi state. In  $\text{FeCl}_2 \cdot 2\text{H}_2\text{O}$ , persisting lines are also observed and have been studied in more detail.<sup>27</sup> It is probable that these lines are due to absorption in areas of the crystal that remain AF, for example, when  $H_0 > H_{C1}$ . These areas, or domains, are not observed at  $6^\circ\text{K}$  and are probably associated with the hysteretic nature of the phase transition at  $H_{C1}$ . They will not be discussed further in this paper.

#### Effects of $\mathcal{J}^L$

The transverse components of the exchange interaction give rise to a term  $\mathcal{J}^L$ , Eq. (8), which adds  $S_i^+ S_{i+\delta}^-$  terms to the Hamiltonian. The major effects of these terms are on the energies of the spin waves or onefold clusters. The simple spin-wave theory<sup>7</sup> shows that  $J^L$  causes the flat Ising band to have dispersion. Thus the  $K=0$  energy, which is measured in our experiments, is shifted downward linearly in  $J^L$ . ( $K$  is the total crystal momentum of the excitation.) We may make a straightforward, but complicated, calculation using conventional spin-wave theory to obtain the spin-wave energies.<sup>2</sup> The onefold cluster excitations are then interpreted as antiferromagnetic resonance (AFMR), ferrimagnetic resonance (FiMR), and ferromagnetic resonance (FMR), in the appropriate region. The resulting frequencies may be expressed in terms of (downward) energy shifts  $\Delta E_i$  from the Ising predictions. (The  $\Delta E_i$  are summarized in the Appendix.) These energy shifts are different for different modes due to the exchange interactions between chains. These (large) effects are evident in the experimental data:  $d_1$  and  $b_1$  are shifted down about  $3 \text{ cm}^{-1}$  more than  $e_1$ , for example.

In the case of the bound-state energies,  $\mathcal{J}^L$  gives rise to only second-order effects. The effects caused by  $J_0^L$ , for example, are discussed in the preceding paper,<sup>6</sup> where it is shown that at  $K=0$  the energy of the  $(n>2)$ -

magnon bound state is reduced by  $(J_0^L)^2/J_0^{zz}$ , while the two-magnon bound-state energy is shifted downward by twice that amount. These shifts ( $\sim 0.3 \text{ cm}^{-1}$ ) are quite small in the case of CC2, due to the large longitudinal anisotropy of this material. [Note added in manuscript. In a recent paper, M. Tachiki, J. Phys. Soc. Japan **26**, 858 (1969), has independently discussed some of the effects of  $\mathcal{J}^L$  and has come to similar conclusions for the energy shifts of the spin-wave and two-magnon bound states.]

The results for the bound states described above were found<sup>6</sup> by considering an isolated ferromagnetic chain, but the linear chains in CC2 (as well as any other crystal) are not isolated; there is some interaction between neighboring chains. The Ising part of this interchain interaction acts like an internal field, which will stabilize the linear chain and give rise to a finite Néel temperature. This effective field  $H_{\text{int}}$  is easily included in the energies, Eq. (10), of the bound states. It is the non-Ising terms, however, which cause spin deviations from one chain to be coupled to deviations on neighboring chains. These interactions may greatly complicate the exact form of the bound states, but as long as  $(J_1^L)^2 \ll 4(J_0^{zz})^2$  the effects on their energies may be neglected. Thus, we take the bound-state energies to be the same as those for an isolated chain acted on by an effective field  $H_0 + H_{\text{int}}$ .

#### Effects of $\mathcal{J}^a$

The transverse anisotropy in the exchange interaction,  $J^a$ , is extremely important in the experiments of  $\text{CoCl}_2 \cdot 2\text{H}_2\text{O}$  (CC2). The term  $\mathcal{J}^a$ , Eq. (9), contains  $S_i^- S_{i+\delta}^-$  and  $S_i^+ S_{i+\delta}^+$  terms, which create or destroy two spin reversals. This is, therefore, a  $\Delta m = \pm 2$  term which can give rise to a coupling between levels with different  $m$  values or different slopes. These effects are most easily described by off-diagonal matrix elements between the states which are coupled.<sup>2,6</sup> For example, a matrix element  $2p_1 J_1^a S$  couples  $a_1$  and  $b_1$ , giving rise to the observed zero-field splitting (as expected from the rhombic symmetry). Similarly, in the Fi state,  $c_1$  and  $d_1$  are coupled by  $\sqrt{2}(p_1 J_1^a + p_2 J_2^a) S$ . All other coupling between chains due to  $\mathcal{J}^a$  is neglected.

The effects of the anisotropic intrachain exchange interactions are well described by the theory developed in the preceding paper.<sup>6</sup> In particular,  $J_0^a$  causes the  $n$ -fold cluster to be coupled to the  $(n+2)$ - and  $(n-2)$ -fold clusters, with an off-diagonal matrix element  $-2J_0^a$  at  $K=0$ . At  $H_{C2}$  the simple Ising model predicts that the clusters in the Fo region are all degenerate, with an energy  $2J_0^{zz}$ , Eq. (11). For finite  $J_0^a$ , these degenerate levels interact and repel, resulting in the formation of a band with a width  $8J_0^a$ . For external fields larger than  $H_{C2}$ , the Ising levels are not degenerate and the interaction is weaker than near  $H_{C2}$  (Fig. 6), giving rise to curvature in the lines. Near  $H_{C2}$  the energy shifts resulting from  $J_0^a$  are approximately  $2 \text{ cm}^{-1}$ , com-

<sup>26</sup> K. A. Hay and J. B. Torrance, Jr., J. Appl. Phys. **40**, 999 (1969).

<sup>27</sup> K. A. Hay and J. B. Torrance, Jr. (to be published).

pared to the  $\sim 0.3 \text{ cm}^{-1}$  shifts in the bound-state energies caused by  $J_0^a$ .

In addition to effects on the *energies* of the bound states,  $\mathfrak{H}^a$  makes it possible to excite these states by electromagnetic radiation in the following way: In order to make a magnetic transition to a level  $|f\rangle$  from the ground state by absorption of radiation, there must exist a nonzero matrix element of  $\mathbf{u} \cdot \mathbf{h}$  between the ground state and the excited state:

$$\langle f | \mathbf{u} \cdot \mathbf{h} | 0 \rangle, \quad (13)$$

where  $\mathbf{u} = \mu_B \mathbf{g} \cdot \mathbf{S}$  and  $\mathbf{h}$  is the oscillating magnetic field of the radiation. In the case of the spin wave or onefold cluster, there is a  $|\Delta m| = 1$  matrix element of  $\mu_x h_x$  at  $K = 0$ :

$$\langle 1 | \mu_x h_x | 0 \rangle = \mu_B g^{xx} h_x \langle 1 | \frac{S^+ + S^-}{2} | 0 \rangle = \frac{\mu_B g^{xx} h_x}{2}.$$

A  $|\Delta m| = 1$  transition can be made, which absorbs the perpendicular component of  $h$ . This is the familiar result of ferromagnetic resonance (FMR).<sup>7</sup>

How can one make a  $\Delta m = 3$  transition to excite the threefold cluster? The transverse anisotropy in the exchange interaction causes some onefold cluster to be admixed into the wave function of the threefold cluster. This admixture is conveniently described by perturbation theory as<sup>2</sup>

$$|3'\rangle = |3\rangle - \frac{(2J_0^a \cos Ka)}{E_3 - E_1} |1\rangle.$$

A matrix element of the form (13) may now be formed at  $K = 0$ :

$$\langle 3' | \mu_x h_x | 0 \rangle = \frac{2J_0^a}{E_3 - E_1} \frac{\mu_B g^{xx} h_x}{2}.$$

Similarly, by higher-order perturbation theory, the fivefold cluster has some onefold cluster admixture, resulting in the following matrix element:

$$\langle 5' | \mu_x h_x | 0 \rangle = \frac{(2J_0^a)^2}{(E_5 - E_3)(E_3 - E_1)} \frac{\mu_B g^{xx} h_x}{2}.$$

Since these matrix elements are proportional to  $h_x$  (or  $h_y$ ), the odd- $n$ -fold clusters should be excited by the magnetic component of the radiation oscillating perpendicular to the axis of magnetization, as is observed. The intensity of absorption is proportional to the square of these matrix elements. Clearly, the smaller the difference in energy between the levels, the larger the admixtures and, hence, the stronger the absorption intensity. At fields much larger than  $H_{C2}$  and with a polarizer which transmits only  $h_x$  or  $h_y$ , only the line  $e_1$  is observed (this is just FMR). As the field is lowered, weak absorption associated with  $e_3$  becomes observable, and near  $H_{C2}$ ,  $e_5$  can be detected, etc. At  $H_{C2}$ , where the levels are highly admixed and form a band, one observes

a band of absorption as all of the odd- $n$ -fold clusters become observable. In this region, the onefold cluster absorption is weakened due to the large admixture of states which are not infrared active.

The coupling between the odd- $n$ -fold clusters is also demonstrated by the interaction with the phonon. The spectrum shown in Fig. 6 clearly shows that the phonon interacts with the odd- $n$ -clusters. The interaction with the spin wave (onefold cluster) is not unreasonable or surprising, but it was at first difficult to imagine exactly how the phonon interacts with the other odd- $n$ -fold clusters. This problem was inadvertently solved by the computer which showed that the observed spectra could be fitted assuming that the phonon interacts directly with the onefold cluster only. But since the onefold cluster is coupled to the other odd- $n$ -fold clusters via  $J_0^a$ , they are indirectly coupled to the phonon, as observed. (Any coupling between the phonon and the even- $n$ -fold clusters was too weak to observe.)

The excitation of even- $n$ -fold clusters is considerably more complicated, due to the coupling of these clusters into the ground state.<sup>2,6</sup> Nevertheless, the effects may be crudely described by perturbation theory. The twofold cluster and ground state are modified by  $J_0^a$ , so that

$$|0'\rangle = |0\rangle + \alpha |2\rangle \quad \text{and} \quad |2'\rangle = |2\rangle - \alpha |0\rangle,$$

where  $\alpha \sim J_0^a/E_2$ . There is now a  $\Delta m = 0$  matrix element:

$$\langle 2' | \mu_x h_x | 0' \rangle = 2\mu_B g_{11} h_x \alpha \sim 2J_0^a \mu_B g_{11} h_x / E_2.$$

Similarly,

$$\langle 4' | \mu_x h_x | 0' \rangle \sim \frac{(2J_0^a)^2}{(E_4 - E_2)E_2} (\mu_B g_{11} h_x).$$

The higher even- $n$ -fold clusters have similar matrix elements. Since all these matrix elements contain  $h_x$ , the even- $n$ -fold clusters should absorb the magnetic component parallel to the axis of magnetization, as is observed. These intensities are largest where the energy denominators are smallest, e.g., near  $H_{C2}$ , except for the twofold cluster whose intensity is not so strongly dependent on field. By comparing the expected intensities for onefold and twofold cluster creation, it is seen that the intensity of the twofold is reduced by  $\alpha^2 \sim (J_0^a/E_2)^2$ , but is enhanced by the ratio of the squares of the  $g$  values,  $(g_{11}/g_1)^2$ . Thus the intensities might be expected to be comparable, as is observed.

Perhaps the most direct evidence of the coupling of the even- $n$ -fold clusters into the ground state is obtained from a measurement of the magnetization: the magnetization is reduced by<sup>2</sup>

$$\frac{\Delta M}{M} \sim \left( \frac{2J_0^a}{E_2} \right)^2.$$

The predicted decrease is  $\sim 1\%$  for  $\text{CoCl}_2 \cdot 2\text{H}_2\text{O}$ . Ex-

perimental measurements of this decrease are not very accurate and vary markedly.<sup>9,12,15,28</sup> Nevertheless, they appear to indicate a somewhat larger decrease than predicted.<sup>2</sup>

### DETAILED COMPARISON OF THEORY AND EXPERIMENT

In this section the results of the preceding sections are combined in order to calculate the theoretical excitation spectrum of spin waves and magnon bound states in  $\text{CoCl}_2 \cdot 2\text{H}_2\text{O}$  (CC2). The complete Hamiltonian is given by (6). The eigenvalues of  $\mathcal{H}^I + \mathcal{H}^L$  are obtained by modifying the Ising results, Eq. (11), to include the downward shifts  $\Delta E_i$  (see Appendix) obtained from the spin-wave calculation and the smaller downward shifts in the bound-state energies due to  $J_0^L$ . These results are summarized below:

AF state:

$$\begin{aligned} h\nu_{a,1} &= 2J_0^{zz} - \Delta E_a + g_{11}\mu_B(H_{C1}' + H_0), \\ h\nu_{a,2} &= 2J_0^{zz}[1 - (j_0^L)^2] + 2g_{11}\mu_B(H_{C1}' + H_0), \\ h\nu_{a,n \geq 3} &= 2J_0^{zz}[1 - (j_0^L)^2/2] + ng_{11}\mu_B(H_{C1}' + H_0), \\ h\nu_{b,1} &= 2J_0^{zz} - \Delta E_b + g_{11}\mu_B(H_{C1}' - H_0), \\ h\nu_{b,2} &= 2J_0^{zz}[1 - (j_0^L)^2] + 2g_{11}\mu_B(H_{C1}' - H_0), \\ h\nu_{b,n \geq 3} &= 2J_0^{zz}[1 - (j_0^L)^2/2] + ng_{11}\mu_B(H_{C1}' - H_0); \end{aligned} \quad (14)$$

Fi state:

$$\begin{aligned} h\nu_{c,1} &= 2J_0^{zz} - \Delta E_c + g_{11}\mu_B H_0, \\ h\nu_{c,2} &= 2J_0^{zz}[1 - (j_0^L)^2] + 2g_{11}\mu_B H_0, \\ h\nu_{c,n \geq 3} &= 2J_0^{zz}[1 - (j_0^L)^2/2] + ng_{11}\mu_B H_0, \\ h\nu_{d,1} &= 2J_0^{zz} - \Delta E_d + g_{11}\mu_B(H_{C2} - H_0), \\ h\nu_{d,2} &= 2J_0^{zz}[1 - (j_0^L)^2] + 2g_{11}\mu_B(H_{C2} - H_0), \\ h\nu_{d,n \geq 3} &= 2J_0^{zz}[1 - (j_0^L)^2/2] + ng_{11}\mu_B(H_{C2} - H_0); \end{aligned} \quad (15)$$

Fo state:

$$\begin{aligned} h\nu_{e,1} &= 2J_0^{zz} - \Delta E_e + g_{11}\mu_B(H_0 - H_{C2}), \\ h\nu_{e,2} &= 2J_0^{zz}[1 - (j_0^L)^2] + 2g_{11}\mu_B(H_0 - H_{C2}), \\ h\nu_{e,n \geq 3} &= 2J_0^{zz}[1 - (j_0^L)^2/2] + ng_{11}\mu_B(H_0 - H_{C2}), \end{aligned} \quad (16)$$

where  $j_0^L \equiv J_0^L/J_0^{zz}$  and where the results for  $n \geq 3$  are valid only for  $(j_0^L)^2 \ll 1$ . Early attempts to fit theory and experiment revealed the necessity of including the (small) effects of the exchange interaction  $J_3$  (Fig. 1) which were previously neglected. Using the Ising model,  $J_3^{zz}$  is found to increase the energy required to create an  $n$ -fold cluster (in all regions) by  $2nJ_3^{zz} = 2ng_{11}\mu_B H_3$ . This increase must be added to each of the energies in (14), (15), and (16). (The effects of  $J_3^L$  and  $J_3^a$  are neglected.) The phonon, with energy  $E_{ph}$ , is also included in each region. These energies form the diagonal elements of the Hamiltonian to be diagonalized.

<sup>28</sup> A. Narath, J. Phys. Soc. Japan **19**, 2244 (1964).

TABLE I. Values of parameters for  $\text{CoCl}_2 \cdot 2\text{H}_2\text{O}$ .

Parameter	Value	Previous value <sup>a</sup>	Source or comment
$g_{11}$	6.81 $\pm$ 0.10	6.77 <sup>b</sup>	Narath (Ref. 18)
$H_{C1}$	31.0 $\pm$ 0.3 kOe	31.3 kOe	Narath (Ref. 14)
$H_{C2}$	44.9 $\pm$ 0.3 kOe	44.9 kOe	Narath (Ref. 14)
$H_3$	0.3 $\pm$ 0.1 kOe	0.7 kOe	Oguchi (Ref. 25)
$J_0^{zz}$	12.66 $\pm$ 0.1 $\text{cm}^{-1}$	6.5 $\text{cm}^{-1e}$	Narath (Ref. 11)
$J_1^{zz}$	-3.25 $\pm$ 0.1 $\text{cm}^{-1}$	6.5 $\text{cm}^{-1e}$	Oguchi (Ref. 25)
$J_2^{zz}$	-0.7 $\pm$ 0.1 $\text{cm}^{-1}$		Obtained from our values of $H_{C1}$ , $H_{C2}$ , and $H_{C3}$ , using (2)
$J_3^{zz}$	0.09 $\pm$ 0.04 $\text{cm}^{-1}$		
$j_0^L$	0.155 $\pm$ 0.01	0.21	Eq. (3) and Ref. 18 <sup>d</sup>
$j_1^L = j_2^L$	0.280 $\pm$ 0.01	0.25	Oguchi (Ref. 25) <sup>d</sup>
$j_0^a$	0.10 $\pm$ 0.01		
$j_1^a = j_2^a$	0.16 $\pm$ 0.02	0.075	Eq. (3) and Ref. 18 <sup>e</sup>
$E_{ph}$	29.3 $\pm$ 0.2 $\text{cm}^{-1}$		...
$A_{AF}^f$	0.55 $\pm$ 0.05 $\text{cm}^{-1}$		...

<sup>a</sup> Previous values are inferred from static susceptibility (Ref. 11) and magnetization (Ref. 14) data.

<sup>b</sup> The often quoted value of 7.3 is obtained from an oversimplified analysis of the susceptibility data.

<sup>c</sup> Indirect estimate.

<sup>d</sup> Assumes  $j_0^L = j_1^L = j_2^L$ .

<sup>e</sup> Assumes  $j_0^a = j_1^a = j_2^a$ .

<sup>f</sup> Magnon-phonon coupling constant in AF state.

The effect of  $\mathcal{H}^a$  is to cause a coupling between these energy levels. These interactions, as well as the phenomenological magnon-phonon coupling, were included as off-diagonal matrix elements between the appropriate levels. Forty eigenfunctions of  $\mathcal{H}^I + \mathcal{H}^L$  were used as basis functions in each region. The resulting  $40 \times 40$  matrix was diagonalized for 600 different values of  $H_0$  with the use of a computer. The results for  $K=0$  were plotted along with the experimental data by a Cal Comp plotter; Figs. 5(a) and 6 show the output of the plotter using the parameters of Table I. The lines represent the theoretical calculations and the points are experimental data. The discussion of the agreement between theory and experiment is conveniently divided into two parts: the results for the magnon bound states ( $n$ -fold cluster,  $n > 1$ ) and those for the spin waves (onefold clusters).

### Results for Bound States

We first consider the case of the bound states, since their energies are determined by fewer parameters than the spin-wave energies. Five parameters ( $J_0^{zz}$ ,  $g_{11}$ ,  $H_{C1}$ ,  $H_{C2}$ , and  $H_3$ ) determine the bound-state eigenvalues of  $\mathcal{H}^I + \mathcal{H}^L$  and a sixth ( $J_0^a$ ) is used to describe the coupling between these levels. (The fit also depends on  $J_0^L$ , but is not very sensitive to this value.) A different choice of  $J_0^{zz}$  would merely shift all the energies up or down. Similarly, the values of  $H_{C1}$ ,  $H_{C2}$ , and  $H_3$  determine the effective "zero" of the abscissa for the five sets of lines. The slope of the lines is determined by the  $g$  value and  $J_0^a$  is used to fit the curvature near  $H_{C2}$  and  $H_{C1}$ . In general, there are enough parameters to expect that the two-magnon bound state, for example, might be roughly fit in each region, even if there were serious faults in the theory itself. The

agreement with the theory is demonstrated by the fact that it not only accurately accounts for the energy of the twofold cluster in all regions, but also the energies of the threefold, fourfold, and even fivefold cluster. Furthermore, the values of the parameters used are reasonable and agree quite well with the expected values; for example, the value of the parameter " $H_{C2}$ " is in agreement with the measured value of the metamagnetic transition field  $H_{C2}$  (see Table I).

In the 20–40-cm<sup>-1</sup> region (Fig. 6) the agreement between theory and experiment for the *bound states* is within 0.3 cm<sup>-1</sup>. Over the entire range of the experimental data [Fig. 5(a)], the agreement is not quite as good. The fit is poorest for the two-magnon bound-state lines  $a_2$  and  $c_2$ .

It is valuable at this point to list the various important approximations made in the theoretical calculations just described for the magnon *bound-state* energies:

(1) All effects of the non-Ising part of the *interchain* exchange interactions are neglected.

(2)  $J_0^a$  causes the bound states to be coupled to states involving two bound states. These effects are neglected.

(3) The values of  $H_{C1}$  and  $H_{C2}$  are related to the exchange interactions  $J_1^{zz}$  and  $J_2^{zz}$  by relations (2) involving the ground-state energies of the metamagnetic phases. The effects of the non-Ising terms on the ground-state energies [and hence on the relations (2)] are neglected. These effects include the antiferromagnetic ground-state problem<sup>7</sup> as well as complications in the ground state caused by  $J_0^a$ .<sup>2</sup>

(4) We also neglect the effect of next-nearest-neighbor interactions, both exchange and dipole-dipole. (The nearest-neighbor part of the dipole-dipole interaction behaves like an effective exchange interaction and is absorbed in the "exchange" constant.)

It is possible that *each* of these effects will give rise to energy shifts of the order of 0.05–0.20 cm<sup>-1</sup>. These contributions make it unrealistic to expect that the theory and experiment can be made to agree better than 0.2 cm<sup>-1</sup> over the entire range of the data.

In addition to the agreement evident in Figs. 5(a) and 6, the values of the parameters used compare favorably with those obtained by others, as is evident from Table I. Furthermore, there are qualitative observations which agree with the theory; for example, the polarization of the radiation absorbed and the general dependence of the intensities on  $n$  and  $H_0$  behave as expected, although quantitative measurements are difficult to obtain. In general, the effects of  $J_0^a$  on the bound-state energies are confirmed. On the other hand, these energies are so weakly dependent on  $J_0^t$  that one can only say that the experimental data are consistent with the theory in the preceding paper<sup>6</sup>; the calculated shifts are of order  $(J_0^t)^2/J_0^{zz} \sim 0.3$  cm<sup>-1</sup>. The spin-wave (or  $n=1$ ) energies, discussed next, give a more sensitive, first-order dependence on  $J_0^t$ .

### Results for Spin Waves

The spin-wave excitations correspond to antiferromagnetic resonance (AFMR), ferrimagnetic resonance (FiMR), and ferromagnetic resonance (FMR) in the appropriate phases. The results of detailed spin-wave calculations<sup>2</sup> for  $\mathfrak{E} = \mathfrak{E}^l + \mathfrak{E}^t$  can be expressed in terms of the shifts  $\Delta E_i$  from the Ising results (see Appendix). These shifts are determined by  $J_0^t$ ,  $J_1^t$ , and  $J_2^t$ . (The effects of  $J_3^t$  are neglected.) When  $\mathfrak{E}^a$ , Eq. (9), is included, it introduces a coupling between  $a_1$  and  $b_1$  and also between  $c_1$  and  $d_1$ . This coupling is in addition to the interaction with the threefold cluster. These latter complications are included as off-diagonal matrix elements, as is the phenomenological magnon-phonon coupling.<sup>26</sup>

Early attempts to fit the data revealed that it is not possible to assume that all the  $j_i^t$  are equal, i.e., it is found that  $J_0^t/J_0^{zz} \neq J_1^t/J_1^{zz}$ . It is also not possible to assume that all the  $j_i^a \neq J_i^a/J_i^{zz}$  are equal. We do assume, however, that  $j_1^t = j_2^t$  and  $j_1^a = j_2^a$ . The spin-wave energies are then determined by three parameters  $j_0^t$ ,  $j_1^t$ , and  $j_1^a$ , in addition to the six used to fit the bound-state energies. Using the values of these parameters shown in Table I, we obtain the spin-wave energies shown by the lines in Figs. 5(a) and 6. There is good agreement between theory and experiment.

The behavior of the resonances at zero field was also examined. The two AFMR resonances are split by  $J_1^a$ , as we would expect from the rhombic crystal field. This anisotropy causes the modes to become elliptical and absorb radiation linearly polarized along the  $x$  and  $y$  directions. Polarization measurements in the  $x$ - $y$  plane confirm this prediction and, in particular, show that  $a_1$  is polarized along an axis which is  $30^\circ \pm 8^\circ$  away from the  $c$  axis in the  $a$ - $c$  plane.<sup>2</sup>

The dipole-dipole interaction between nearest-neighbor spins contributes to the effective exchange interaction, Eq. (5). The exact nature of this contribution is complicated in this case because the moments are anisotropic and because the nearest-neighbor distance is different in different directions. Since the magnitude of this effect is  $\sim 0.5$  cm<sup>-1</sup>, it is expected that the dipole-dipole interaction has important effects on the values of  $j_0^t$ ,  $j_0^a$ ,  $j_1^t$ , and  $j_1^a$  (Table I). This interaction may, for example, be largely responsible for why  $j_1^t \neq j_0^t$ .

### CONCLUSION AND GENERAL DISCUSSION

The linear ferromagnetic chains of  $\text{CoCl}_2 \cdot 2\text{H}_2\text{O}$  (CC2) are in different magnetic environments in the three metamagnetic phases of this material. In each of these environments multiple-magnon bound states, involving up to five magnons, have been observed in these chains. The measured energy spectrum is in excellent agreement with the theoretical spectrum, which is obtained by the method developed in the preceding paper.<sup>6</sup>

The importance of such bound states was recognized by Bethe as early as 1931.<sup>4</sup> Wortis<sup>5</sup> has shown that two-magnon bound states exist in all ferromagnets. How, then, have bound states escaped direct observation until the present work? The reason for this difficulty is that in a typical magnetic material the two-magnon bound state exists only near the edge of the Brillouin zone, i.e., only in that region of  $K$  space does the bound-state energy lie below the energy band formed by two unbound magnons with the same total  $K$ .<sup>5,6</sup> For this reason, magnon bound states are extremely difficult to observe experimentally: Thermodynamic measurements are dominated by the overwhelming statistical weight of unbound magnons, and spectroscopic investigations usually probe the region near  $K=0$ , where bound states generally do not exist. Even in cases where they do exist at  $K=0$ , the transition is usually forbidden. For inelastic neutron scattering, the cross section of bound states is predicted to be two orders of magnitude less than that for the spin waves.<sup>29</sup>

What are the properties of CC2 that make the observation of bound states possible in this material? In general, there are three major factors that affect the existence of bound states<sup>6</sup>: (1) the magnitude of the spin  $S$ ; (2) the number  $p$  of nearest neighbors; and (3) the longitudinal anisotropy. The two-magnon bound state exists in a larger volume of  $K$  space for materials with: (1) lower  $S$ ; (2) lower  $p$ ; and (3) larger longitudinal anisotropy. In fact, in CC2 where  $S=\frac{1}{2}$ ,  $p=2$  (linear chain), and there is large longitudinal anisotropy, the two-magnon bound state exists throughout  $K$  space, including  $K=0$ . Furthermore, in CC2 the transverse anisotropy in the exchange interaction relaxes the  $\Delta m=\pm 1$  selection rule so that bound states may be excited at  $K=0$  by photon absorption. The conditions for the existence of  $n$ -magnon bound states for  $n>2$  are much more restrictive than for  $n=2$ . It is highly unlikely that these states would be observable except in an  $S=\frac{1}{2}$ , linear-chain spin system with large longitudinal anisotropy.

There have been *indirect* observations of magnon bound states in ordered magnetic materials: Date and Motokawa<sup>3</sup> have observed microwave absorption in CC2 which is associated with a transition between a thermally excited spin wave and the two-magnon bound state, as well as transitions between different bound states. This absorption is called spin cluster resonance. Date and Motokawa developed the simple Ising model of CC2 to describe their results. Spin cluster resonance is equivalent to the central line of the triplet structure that has recently been observed in the optical experiments of Hufner *et al.*<sup>30</sup> These indirect measurements might be difficult to analyze in detail, since they contain contributions from the entire Brillouin

zone. Recently, other possible indirect methods of observing bound states have been proposed.<sup>29,31</sup>

It is valuable at this point to compare  $\text{CoCl}_2 \cdot 2\text{H}_2\text{O}$  (CC2) with  $\text{FeCl}_2 \cdot 2\text{H}_2\text{O}$  (FC2). Since these crystals are isomorphic and have nearly identical lattice spacings<sup>32</sup> and ionic masses, many of their properties are expected to be similar. For example, a low-lying optical phonon at about  $30 \text{ cm}^{-1}$  is observed in each material,<sup>26</sup> as well as the onset of strong (presumably) optical phonon absorption at  $\sim 145 \text{ cm}^{-1}$ .<sup>27</sup> The Néel temperatures ( $17.2$  and  $23^\circ\text{K}$ ) and metamagnetic behavior of CC2 and FC2 are also similar, with comparable values of  $H_{C1}$  (31 and 39 kOe) and  $H_{C2}$  (44.9 kOe for both).<sup>33</sup> The magnetic structures (Fig. 1) are the same except that the axis of magnetization of FC2 is in the  $a$ - $c$  plane. The large longitudinal anisotropy of both crystals gives rise to high energy ( $\sim 30 \text{ cm}^{-1}$ ) spin-wave resonance frequencies. Although the general features of the *spin-wave* spectra are quite similar, a detailed examination reveals differences due to the different properties of the  $\text{Fe}^{2+}$  and  $\text{Co}^{2+}$  spins. In the  $\text{Fe}^{2+}$  case, the spectrum is well described by  $S=2$  (free ion spin),  $g=2.23$ , and an isotropic exchange interaction.<sup>27</sup> The (large) anisotropy appears uniaxial and is contained in a single-ion crystal-field anisotropy (i.e., a  $DS_z^2$  term, with  $D \approx -9.6 \text{ cm}^{-1}$ ). In CC2, on the other hand, the anisotropy is so large that it is convenient to make a transformation to a fictitious spin  $S=\frac{1}{2}$  (the free-ion value is  $\frac{3}{2}$ ) and to include the anisotropy in effective exchange and  $g$  tensors.

In spite of these differences in the magnetic properties, the spin-wave spectra of these salts are remarkably similar. The bound-state spectra, however, are expected to be quite different. Although FC2 contains linear chains ( $p=2$ ) and has strong longitudinal anisotropy, the difference in the magnitude of the spin and form of the anisotropy are expected to give rise to a bound-state spectrum significantly different from that observed in CC2. Unfortunately, in FC2,  $J_0^a \sim 0$  (i.e., the anisotropy is uniaxial) and it is not possible to excite the bound states as in the case of CC2. The theoretical predictions concerning the bound-state spectrum therefore could not be verified as no absorption was observed apart from that due to  $n=1$  spin-wave excitations.

In the isomorphic compound  $\text{CoBr}_2 \cdot 2\text{H}_2\text{O}$  (CB2) the lattice constants are significantly different from FC2 and CC2. In this crystal the magnetic interactions are weaker, resulting in a lower Néel temperature ( $9^\circ\text{K}$ ) and smaller values of  $H_{C1}$  (13.7 kOe) and  $H_{C2}$  (29.8 kOe).<sup>28</sup> The spin-wave spectrum is qualitatively similar to FC2 and CC2, but with lower energies ( $\sim 20 \text{ cm}^{-1}$ ).<sup>34</sup> In this case the  $\text{Co}^{2+}$  ion behaves like that in CC2, with

<sup>29</sup> R. Silbergliitt, J. Appl. Phys. **40**, 1114 (1969).

<sup>30</sup> B. Morosin and E. J. Graeber, J. Chem. Phys. **42**, 898 (1965).

<sup>31</sup> A. Narath, Phys. Rev. **139**, A1221 (1965).

<sup>32</sup> J. B. Torrance, Jr., and K. A. Hay (unpublished); also Ref. 2.

<sup>29</sup> R. Silbergliitt and A. B. Harris, Phys. Rev. **174**, 640 (1968).

<sup>30</sup> S. Hufner, L. Holmes, F. Varsanyi, and L. G. Van Uitert, Phys. Rev. **171**, 507 (1968).

large rhombic exchange anisotropy and  $S=\frac{1}{2}$ . For this reason, bound states similar to those observed in CC2 are observed in CB2.<sup>34</sup>

#### ACKNOWLEDGMENT

The authors have benefited from helpful discussions with Dr. K. A. Hay.

#### APPENDIX

The calculation of the spin wave energies is complicated, but straightforward.<sup>2</sup> The resulting energies at  $K=0$  for  $3C^I+3C^I$  are less than the energies for  $3C^I$  alone, i.e., less than the Ising energies, Eq. (11), for  $n=1$ . The differences  $\Delta E_i$  in energy caused by  $3C^I$  are summarized below:

$$\Delta E_a = \Delta E_b = p_0 J_{0^1} - p_2 |J_{2^1}| + \frac{\frac{1}{2}(p_1 J_{1^1})^2}{p_0(J_{0^{zz}} - J_{0^1}) + p_1 |J_{1^{zz}} - J_{1^1}| - p_2 |J_{2^{zz}} - J_{2^1}|},$$

$$\Delta E_c = p_0 J_{0^1} - \frac{1}{2}(p_1 |J_{1^1}| + p_2 |J_{2^1}|) + B,$$

$$\Delta E_d = p_0 J_{0^1} + B,$$

$$\Delta E_e = p_0 J_{0^1} - p_1 |J_{1^{zz}}| - p_2 |J_{2^{zz}}|,$$

where

$$B = \frac{(p_1 |J_{1^1}| + p_2 |J_{2^1}|)^2}{4p_0(J_{0^{zz}} - J_{0^1}) + 2(p_1 |J_{1^{zz}}| + p_2 |J_{2^{zz}}|) + (p_1 |J_{1^1}| - p_2 |J_{2^1}|)}.$$

These results are used in the theoretical calculations whose results are shown in Figs. 5(a) and 6.

### Magnetic Properties of Plutonium Monophosphide†

D. J. LAM, F. Y. FRADIN, AND O. L. KRUGER\*

Argonne National Laboratory, Argonne, Illinois 60439

(Received 4 June 1969)

The results of magnetization and NMR measurements of plutonium monophosphide are reported. A paramagnetic moment of  $1.06\mu_B$  was obtained from the  $\chi^{-1}$ -versus- $T$  plot, above the Curie temperature of  $126^\circ\text{K}$ , after subtracting a value of  $190 \times 10^{-6}$  emu/mole for the temperature-independent orbital paramagnetism. A ferromagnetic moment of  $0.42\mu_B$  per formula unit was obtained for PuP. The Knight shift of  $P^{31}$  in PuP is linearly dependent on the magnetic susceptibility above the Curie temperature. An effective hyperfine field of  $-51$  kG was determined from the slope of the  $K$ -versus- $\chi$  curve. The relaxation rate can be described in terms of the Knight shift  $K = K_{\text{PuP}} - K_{\text{ThP}}$  by  $\{(T_1 T)^{-1} = (23.5 \pm 1.7) \times 10^6 K (\text{sec } ^\circ\text{K})^{-1}$ . The saturation moment is discussed in terms of the localized- $5f$ -electron model, and the NMR results are discussed in terms of the coupling of the conduction electrons and the localized  $5f$  electrons.

#### I. INTRODUCTION

EXPERIMENTAL studies of the magnetic properties of NaCl-type actinide compounds with group IV A, V A, and VI A elements have concentrated mainly on uranium compounds. The compound UC of uranium with the group IV A element carbon is paramagnetic, all compounds with the group V A elements order antiferromagnetically, and compounds with the group VI A elements S, Se, and Te order ferromagnetically. This simple systematic dependence of the magnetic ordering on the alloying-element group is useful for theoretical interpretation. Indeed, Grunzweig-Genossar, Kuznietz, and Friedman<sup>1</sup> recently pro-

posed a model based on the Ruderman-Kittel-Kasuya-Yosida (RKKY), coupling mechanism to correlate and explain the magnetic interactions of all the NaCl-type uranium compounds with group V A and VI A elements. Since only limited information on the magnetic properties of NaCl-type compounds of neptunium and plutonium has been published,<sup>2-5</sup> it is difficult to evaluate the applicability of the model of Ref. 1 to NaCl-type compounds of heavier actinides. In this paper we report the results of magnetic-susceptibility,

<sup>2</sup> D. J. Lam, M. V. Nevitt, J. W. Ross, and A. W. Mitchell, *Plutonium 1965*, edited by A. G. Kay and M. B. Waldron (Chapman and Hall, Ltd., London, 1967), p. 274; J. W. Ross and D. J. Lam, *J. Appl. Phys.* **39**, 1451 (1967).

<sup>3</sup> R. Lallemand, P. Costa, and R. Pascard, *J. Phys. Chem. Solids* **26**, 1255 (1965); C. H. De Novion, and R. Lorenzelli, *ibid.* **29**, 1901 (1968).

<sup>4</sup> G. H. Lander, L. Heaton, M. H. Mueller, and K. D. Anderson, *J. Phys. Chem. Solids* **30**, 733 (1969).

<sup>5</sup> B. D. Dunlap, M. B. Brodsky, G. M. Kalvius, G. K. Shenoy, and D. J. Lam, *J. Appl. Phys.* **40**, 1495 (1969).

† Work performed under the auspices of the U. S. Atomic Energy Commission.

\* Present address: Battelle Memorial Intsitute, Columbus, Ohio.

<sup>1</sup> J. Grunzweig-Genossar, M. Kuznietz, and F. Friedman, *Phys. Rev.* **173**, 562 (1968).